Journal of Cerebral Blood Flow and Metabolism
16:720–728 © 1996 The International Society of Cerebral Blood Flow and Metabolism
Published by Lippincott–Raven Publishers, Philadelphia

Local Cerebral Blood Flow in a Rat Cortical Vein Occlusion Model

H. Nakase, A. Heimann, and O. Kempski

Institute for Neurosurgical Pathophysiology, Johannes Gutenberg University Mainz, Mainz, Germany

Summary: The symptoms following sinus and vein occlusion observed in patients and experimental animals display a considerable variability that so far remains largely unexplained. In a rat cortical vein occlusion model using a photochemical thrombotic technique, we examined changes in the cerebral venous flow pattern by fluorescence angiography and regional cerebral blood flow (rCBF) and cerebral blood volume fraction (CBVF) by a modern laser Doppler "scanning" technique. Brain damage was assessed histologically. Fluorescence angiographic findings fell into two groups: group A, rats with an altered venous flow pattern after occlusion (n = 12), and group B, rats with interruption of blood flow and/or a growing venous thrombus (n = 5). In addition, sham-operated animals made up group C (n = 5). Extravasation of fluorescein, a massive decrease in rCBF, a short-lasting increase in CBVF, and regional brain damage were typical for group B. In addition, cortical CBF mapping revealed a transient hyperperfusion zone with hyperemia surrounding a hypoperfused ischemic core in group B. A circulation perturbation following venous occlusion appeared near those occluded cerebral veins without sufficient collateral flow. Furthermore, the venous thrombus continued to grow, accompanied by local critical ischemia and severe brain damage. Conversely, 71% of the animals (12 of 17) tolerated occlusion of a solitary vein without major flow disturbances or histological evidence of damage to the CNS (group A). **Key Words:** Cerebral blood flow—Vein occlusion—Microcirculation—Laser Doppler flowmetry—Fluorescence angiography—Rose bengal photothrombosis.

The clinical symptoms and prognosis of cerebral sinus vein thrombosis (SVT) and intraoperative occlusion of cerebral veins are well-known to be quite variable, ranging from no symptoms at all to severe venous infarction. The pathophysiological mechanisms underlying this high variability in patients and experimental animals are unknown and among the main topics of interest in this field (Fries et al., 1992; Gotoh et al., 1993; Ungersböck et al., 1993*a*).

Much attention has been paid to the study of cerebral injury following venous circulation disturbances (Cervos-Navarro and Kannuki, 1990; Takeshima et al., 1993; Frerichs et al., 1994). Neurosurgical operations are performed more frequently in elderly patients, and mild venous circulation disturbances, which are without consequence in young patients, often cause unexpectedly severe complications in the elderly. Also, extensive operations, such as skull base surgery, have become routine in neurosurgery, and sinuses and bridging veins are often exposed, increasing risk of postoperative complications following interruption of the venous circulation (Kanno et al., 1992). Unfortunately, very little information is available on the pathophysiology of venous circulation disturbances in the brain. The main reasons for this knowledge deficit are the primary focus of experimental studies on arterial occlusion, the frequent anatomical variations in the cerebral venous system, and the technically challenging experimental procedures necessary to occlude sinus and veins in small animals.

Experiments on SVT have demonstrated that occlusion of the superior sagittal sinus (SSS) alone is not sufficient to block venous outflow and that a cerebral venous thrombosis becomes critical for the parenchymal blood supply only if draining cortical veins are occluded (Fries et al., 1992; Gotoh et al., 1993; Ungersböck et al., 1993*a*). These experi-

Received June 5, 1995; final revision received November 3, 1995; accepted November 3, 1995.

Address correspondence and reprint requests to Dr. Oliver Kempski, Institute for Neurosurgical Pathophysiology, Johannes Gutenberg University Mainz, 55101 Mainz, Germany.

Abbreviations used: ANOVA, analysis of variance; CBVF, cerebral blood volume fraction; lCBF, local cerebral blood flow; LD, laser Doppler; rCBF, regional cerebral blood flow; SSS, superior sagittal sinus; SVT, sinus vein thrombosis.

ments, however, could not satisfactorily explain the mechanisms behind the various symptoms after venous occlusion. For instance, in a rat model of SVT, different investigators found very similar percentages of animals with histological damage without being able to identify in detail the processes necessary to cause thrombosis progression in some animals (Ungersböck et al., 1993*a;* Frerichs et al., 1994).

We have devised a new, less invasive, and clinically relevant model of rat cortical vein occlusion by a photochemical thrombotic technique, which is characterized by a high variety of symptoms following occlusion of a single vein and reproducible brain damage (90%) after occlusion of two adjacent veins (Nakase et al., 1995). Therefore, the occlusion of a single vein is a model suited for studies of the variable pathophysiology of venous occlusion observed experimentally as well as in patients. An advanced laser Doppler (LD) "scanning" technique, in which the LD probe is moved about by a computer-controlled motor-driven micromanipulator to multiple defined positions in the cranial window (Heimann et al., 1994; Kempski et al., 1995), was used to determine local cerebral blood flow (lCBF) in many different adjacent locations. The resultant data can be used to calculate representative regional cerebral blood flow (rCBF) histograms and to perform cortical CBF mapping, which are not possible with single-point LD measurements (Ungersböck et al., 1993*b;* Heimann et al., 1994).

The current experiment was designed to examine early lCBF changes after venous occlusion, which may serve as early indicators of the variability of clinical symptoms. We examined the flow pattern and growth of a venous thrombosis by fluorescence angiography, rCBF and cerebral blood volume fraction (CBVF) by LD scanning, and brain damage histologically in a single-cortical-vein occlusion model using rose bengal for photochemical thrombosis induction.

METHODS

Animal preparation

Twenty-four male Wistar rats (260–360 g) were premedicated with 0.5 mg atropine. Anesthesia was introduced with ether and continued by i.p. injection of chloral hydrate (36 mg/100 g body weight). During the experiment, spontaneous ventilation was maintained, and rectal temperature was kept at 37°C by means of a feedback-controlled homeothermic blanket control unit (Harvard, South Natick, MA, U.S.A.). Polyethylene catheters were inserted into the tail artery and the right femoral vein. The arterial line allowed continuous registration of arterial blood pressure and blood gas analysis, and the venous lines allowed administration of fluid and drugs. P_aO_2, P_aCO_2, and arterial pH were measured using an ABL3 blood gas analyzer (Radiometer, Copenhagen, Denmark). Blood pressure was continuously monitored through the intraarterial catheter connected to a pressure transducer (Gould 134615-50). Each rat was mounted in a stereotactic frame (Stoelting, Wood Dale, IL, U.S.A.). After a 1.5-cm midline skin incision was made, a cranial window (4.5 × 6 mm) was made over the right frontoparietal region (2 mm lateral and 1 mm caudal to the bregma) by a high-speed drill under an operating microscope (OP-Microscope, Zeiss, Wetzlar, Germany). During the craniotomy, the drill tip was cooled continuously with physiological saline to avoid thermal injury to the cortex. The dura was left intact, and the right frontoparietal cortex was exposed.

Fluorescence angiography

Fluorescence angiography was performed to examine epicortical vessel structures. After i.v. injection of 0.1 ml of 2% Na^+–fluorescein solution (E. Merck, Darmstadt, Germany), fluorescence emission of the brain surface was studied by using an excitation source at a wavelength of 450–490 nm (I2 filter block, Leitz, Wetzlar, Germany). A photomacroscope with magnification from ×5.8 to ×35 (M420, Wild, Heerbrugg, Switzerland), furnished with a 50-W mercury lamp and fluorescence filter, was used for fluorescence angiography, which was carried out before and 30 and 90 min after induction of venous occlusion. The images were recorded on videotape [HS-S5600E(RS), Mitsubishi, Japan], permitting off-line reevaluation. To minimize damage by fluorescence excitation or environmental light, illumination of dura and underlying cortex was restricted to angiography.

CBVF and lCBF measurement

lCBF was measured by a TSI laser flow blood perfusion monitor (model BPM 403a, TSI, St. Paul, MN, U.S.A.) using a 0.8-mm needle probe. CBVF and lCBF were expressed in arbitrary units and LD units, respectively. The lCBF was measured over the intact dura at 48 locations (8 × 6) in a scanning procedure by means of a computer-controlled motor-driven micromanipulator with the occluded vein central to the scanning field in 15-min intervals for 90 min after occlusion (Fig. 1). Thus, the random registration of 48 individual measurements resulted in one scanning procedure with information from 48 different locations, each at a distance of 400 μm. The TSI laser Doppler provides lCBF information that—although not calibrated in absolute units—has a stable and low biological zero (Kempski et al., 1995). CBVF data in essence describe the fraction of moving particles (cells) as compared with the fixed structures of the cerebral parenchyma.

Cortical vein occlusion by photochemical thrombotic technique

A stock solution of rose bengal (Sigma, St. Louis, MO, U.S.A.), 30 mg/ml in 0.9% saline, was prepared for i.v. injection through the femoral vein at a dose of 50 mg/kg. Illumination of the right cortical vein was begun immediately after i.v. injection of the rose bengal solution at 20 mg/kg/min. Special care was taken to avoid illumination of tissue and other vessels adjacent to the vein. Transillumination of green light was achieved by using a 50-W mercury lamp (5,000–6,000 lx, 540 nm) connected to a 100-μm fiber optic that was selectively pointed to a pre-

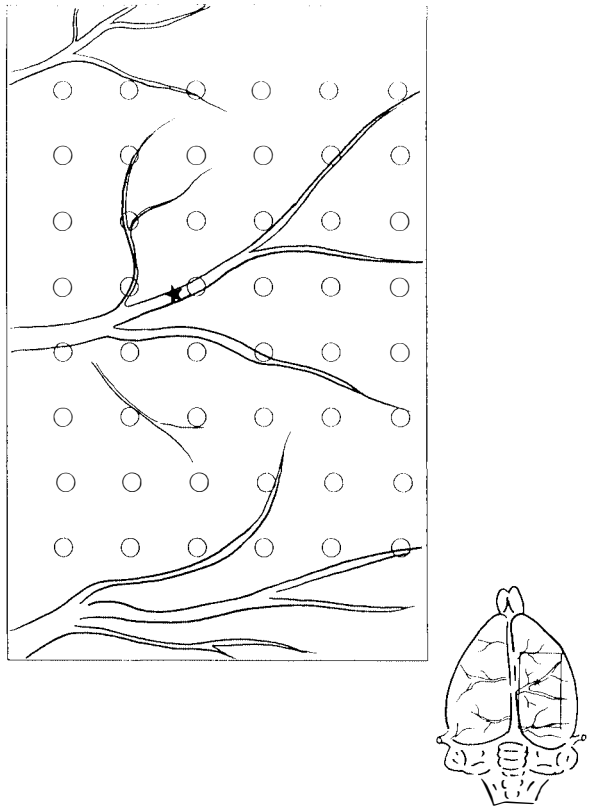

FIG. 1. Schematic drawing demonstrates the point of the occlusion of cortical vein and 48 locations used in a scanning procedure with a computer-controlled micromanipulator. The occluded point of the veins is indicated by an asterisk.

defined location over the target vein for 10 min. The completeness of the occlusion of the cortical vein was confirmed later by fluorescence angiography.

Experimental protocol

After thrombosis induction, the multiple LD scanning was repeated every 15 min for 90 min. After the third fluorescence angiography, the resected bone flap was repositioned and the skin wounds were closed. The rats were returned to individual cages and allowed free access to water and food. Two days after surgery, the rats were observed for clinical manifestations and received an injection of 2.0% Evans blue solution (1 ml/kg) under general anesthesia with chloral hydrate. After 1 h, the rats were submitted to perfusion fixation with 4% paraformaldehyde, and the brains were removed from the skull. Brains were embedded in paraffin to obtain coronal sections of the frontal region, and sections were stained with hematoxylin–eosin. In 19 rats, the cortical vein was occluded by the photochemical thrombotic technique according to the procedure already described. In addition, five rats served as sham-operated controls. These animals received a craniotomy, injection of the rose bengal solution, and a series of fluorescence angiographies, but no fiber optic illumination.

Cortical CBF mapping

For the cortical CBF mapping, CBF data from 48 predefined locations were expressed as percentages of change from the individual preocclusion baselines. CBF data were correlated to the topographical situation in the cranial window and then arranged in a three-dimensional image using xyz triplet columns for a mesh plot. The z-axis expressed percentage changes of lCBF as compared with the initial control values.

Statistical analysis

Data are expressed as means ± SD for physiological variables and as means ± SD of the medians of the 48 lCBF and CBVF values found in each rat. The Mann–Whitney *U* test was used for physiological variables such as blood gases and mean arterial blood pressure. Differences in rCBF and CBVF were evaluated by analysis of variance (ANOVA) (Dunnet's test) for repeated measures and by the Kruskal–Wallis test with multiple comparisons for between-group comparisons. Statistical significance was accepted at an error probability of $p < 0.05$. All statistics were done by Sigma-Stat software (Jandel Scientific, Erkrath, Germany).

RESULTS

Fluorescence angiographical findings

Complete occlusion of the targeted cortical vein, with other vessels undamaged around the irradiation point on the second fluorescence angiography, was achieved in 17 rats (Fig. 2). In two other rats the primary occlusion was incomplete, so these cases were omitted from the study.

Fluorescence angiography provided information about the direction of flow and the extension of the thrombus of the occluded vein. According to the pattern of the angiographic findings, animals could be divided into two groups: group A, which showed only alterations of venous flow without venous stasis (n = 12), and group B, in which interruption of venous blood flow beyond the occlusion point and/or growing venous thrombus was observed (n = 5). A third group (group C, n = 5) consisted of sham-operated animals that received rose bengal but no illumination to induce venous thrombus formation.

In the second angiography, the distal venous flow reversed in direction without circulation stoppage in group A. In group B, flow reversal dilatation of the distal portion of the occluded vein, and deceleration of flow were observed (Fig. 3A). In two of five animals from group B, oscillating flow was seen. The third angiography verified an arrest of flow and further extension of the thrombus only in group B (Fig. 3B). An extravasation of fluorescein into the parenchyma close to the occluded vein was recognized both in group A (two rats) and in group B (all five rats). Sham-operated controls (group C) had no occlusion of the vessels and no extravasation of fluorescein.

Physiological variables

Physiological variables showed no significant changes in blood gases (P_aO_2, P_aCO_2, and hemoglobin; Table 1) and MABP (Table 2) before and after

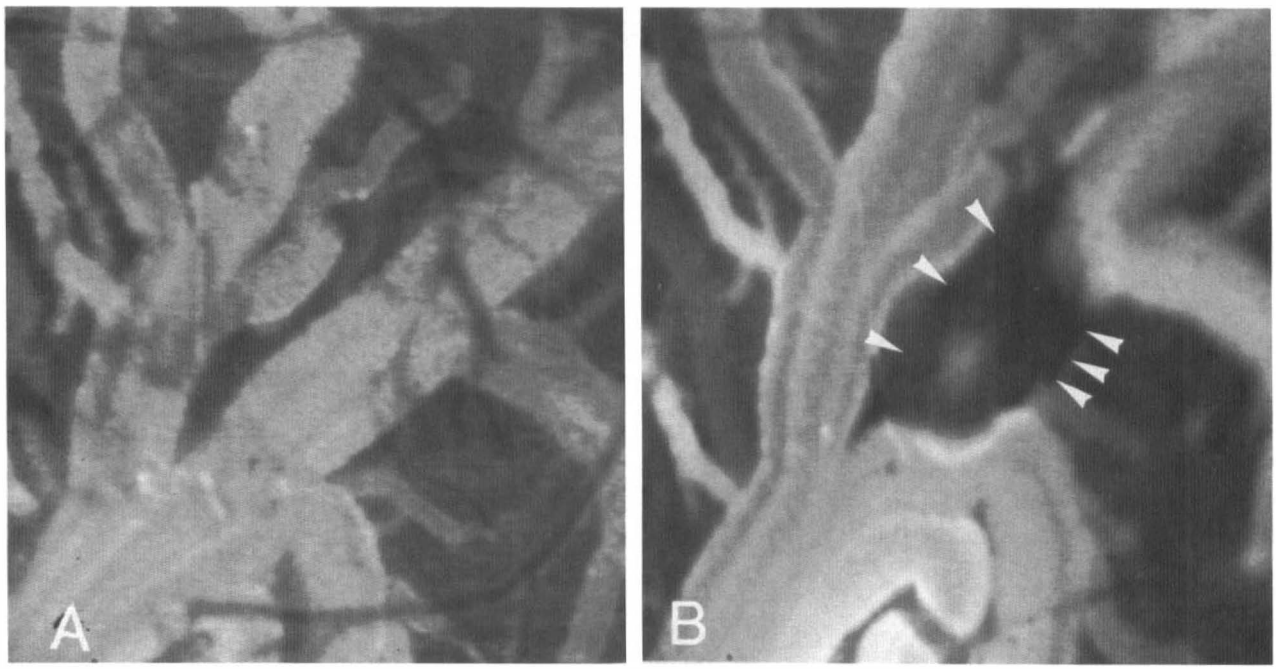

FIG. 2. Fluorescence angiography of the target vein before **(A)** and after **(B)** occlusion using the photochemical thrombotic technique. Arrowheads indicate the occlusion site (original magnification, ×30).

venous occlusion; there were no significant differences in these variables between groups.

CBVF and rCBF

The calculation of median rCBF and CBVF values for the 48 locations in each animal revealed no changes in groups A and C and a transient increase of CBVF in four group B rats (30 min after occlusion, $p < 0.05$; Fig. 4), followed by a massive decrease in rCBF 60, 75, and 90 min after occlusion ($p < 0.05$; Fig. 5). Significant differences were observed between groups A and B at 60, 75, and 90 min after occlusion in rCBF (Fig. 5) and at 30 min after occlusion in CBVF (Fig. 4).

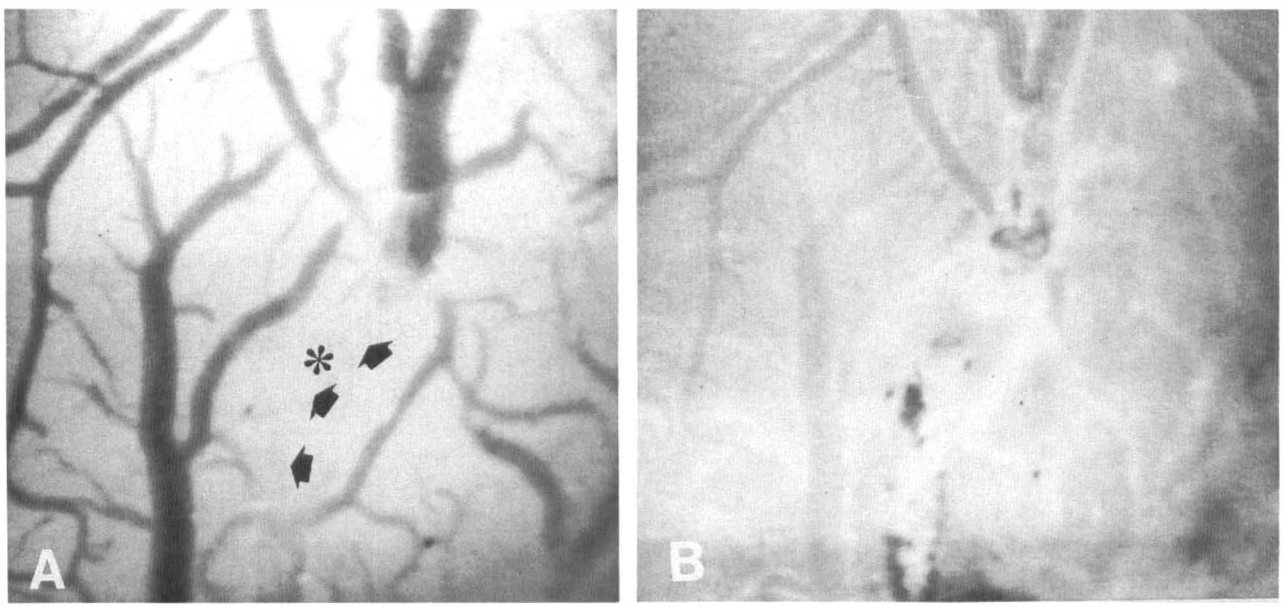

FIG. 3. A: Fluorescence angiography 30 min after thrombus induction in animal no. 6. The photochemically induced thrombus is marked by an asterisk, and the growth of thrombus is indicated by arrows. The venous thrombus is still growing at this time point, and the distal portion of the occluded vein is dilated (original magnification, ×16). **B:** Fluorescence angiography 90 min after thrombus induction of the same rat shows extensive growth of the thrombus and considerable extravasation of fluorescein (original magnification, ×16).

TABLE 1. *Arterial blood gas values before and after occlusion*

Group	Before			After		
	Po_2	Pco_2	Hb	Po_2	Pco_2	Hb
A	83.5 ± 7.1	43.9 ± 3.0	19.3 ± 0.5	86.4 ± 7.5	45.8 ± 3.7	19.2 ± 0.9
B	83.2 ± 7.7	44.0 ± 2.6	19.2 ± 0.4	86.6 ± 6.5	45.3 ± 3.2	19.2 ± 0.7
C	81.5 ± 3.4	45.8 ± 5.6	19.3 ± 1.1	80.1 ± 8.0	45.1 ± 3.1	18.3 ± 1.2

Values are means ± SD; Po_2, mm Hg; Pco_2, mm Hg; Hb (hemoglobin), g/dl. There were no statistical differences between any of the groups before and after injection by ANOVA at $p = 0.05$.

Cortical CBF mapping

Cortical CBF mapping proved that cortical vein occlusion in many cases is tolerated without any lasting change in rCBF, as seen in group A (Fig. 6). In group B, however, a transient hyperperfusion zone with initial hyperemia around a hypoperfused core was found in three of five animals. With growth of the thrombus, blood flow to the core diminished to 15–20% of the initial flow values (Fig. 7). This protracted flow reduction was witnessed in all five rats of group B.

Clinical observations and histology

After 2 days, none of the experimental animals had died or had developed any obvious focal neurological symptoms following cortical vein occlusion or sham-operation. Macroscopic and histopathological examinations demonstrated that the brains of the sham-operated control animals (group C) appeared normal. Neither hemorrhage nor Evans blue extravasation were detected. In group A, light microscopic examination showed parenchymal damage, including vasogenic edema with extravasation of Evans blue in one rat, slight edematous changes with an enlarged extracellular space and tissue pallor and no extravasation of dye in two rats, and normal histological findings in the other nine rats. In group B, all five rats had parenchymal damage, with multiple petechial hemorrhages surrounding the dilated capillaries (one rat), extensive edematous areas in the white and gray matter with extravasation of Evans blue, and disseminated small areas of infarction (all rats). Unfortunately, with the current techniques it was not possible to correlate histopathological damage topographically to the rCBF changes detected.

DISCUSSION

There have been several reports on SVT using various animal models, and each set of authors has mentioned the characteristic inconsistency of brain damage after SVT (Beck and Russell, 1946; Sato et al., 1985; Cervos-Navarro and Kannuki, 1990; Tsujimoto, 1990; Fries et al., 1992; Gotoh et al,. 1993; Takeshima et al., 1993; Ungersböck et al., 1993*a;* Frerichs et al., 1994). Most of the previous studies of SVT employed direct manipulations of the SSS using ligation, ballooning, coagulation, and/or injection of obstructing or thrombotic materials. We found no report of direct thrombosis induction in cortical veins except for our own previous communication (Nakase et al., 1995). A model of more distal and selective venous occlusion is needed to eliminate a factor of variability typical for the venous drainage system: that is, the sole occlusion of central veins such as sinuses or bridging veins permits venous outflow via collateral pathways.

Our newly developed model of cerebral venous occlusion using a photochemical dye has distinct advantages. First, it does not influence physiological variables such as blood pressure, pulse, blood gases, and hematocrit (Nakase et al., 1995); this is an important factor, particularly in small experimental animals, and it facilitates survival. Second, the model has few local side effects; thrombotic occlusion is produced by aggregating platelets and the vessel surface exhibits no evidence of injury (Nakayama et al., 1988; Watson et al., 1987). We have verified these findings by repeated histological studies and by use of cultured endothelial cells exposed to dye and light (data not shown).

Illumination per se has been confirmed to cause

TABLE 2. *Arterial blood pressures*

Group	Baseline	Time intervals during experiment (min)					
		15	30	45	60	75	90
A	80.0 ± 6.0	82.9 ± 7.3	82.2 ± 8.6	82.4 ± 6.7	81.1 ± 7.1	81.1 ± 8.3	78.9 ± 7.2
B	82.3 ± 10.1	79.8 ± 11.3	79.8 ± 10.7	81.2 ± 8.3	79.4 ± 7.8	80.5 ± 11.8	80.3 ± 14.1
C	83.2 ± 4.8	85.3 ± 10.6	84.6 ± 10.2	82.4 ± 5.8	80.8 ± 6.9	81.6 ± 10.2	81.4 ± 9.1

Values are means ± SD. There were no statistical differences between any of the groups by ANOVA at $p = 0.05$.

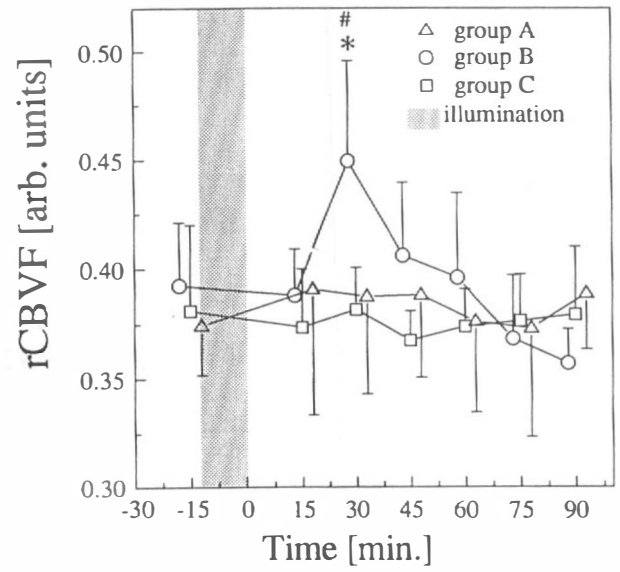

FIG. 4. Graph shows sequential changes in CBVF, expressed in arbitrary units (mean ± SD of median CBVF from 48 locations in each animal). Transient elevation of CBVF was seen 30 min after occlusion (*, $p < 0.05$; 30 min after occlusion). Significant difference between groups A and B is indicated by ($p < 0.05$; 30 min after occlusion).

no brain damage. Direct manipulation of intracranial vessels is not required, and thrombosis can be induced without damage to the dura. With rose bengal, however, the brain is sensitive to 500–600-nm wavelength light and should be protected against these wavelengths for at least 30 min. Much care

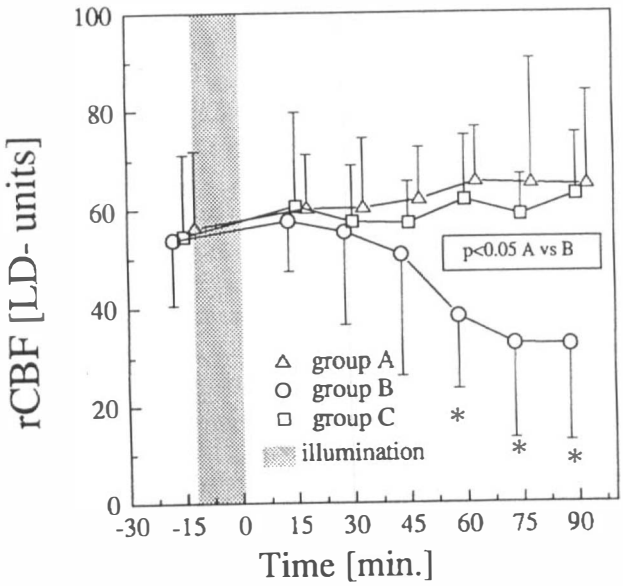

FIG. 5. Graph shows sequential changes in rCBF, expressed in LD units (means ± SD of median lCBF from 48 locations in each animal). In group B, rCBF significantly decreased 60, 75, and 90 min after occlusion (*, $p < 0.05$). Significant differences between groups A and B are indicated by the bar (60, 75, and 90 min after occlusion, ≠, $p < 0.05$).

should be taken to avoid illumination of tissue and other vessels next to the target vein. Therefore, confirmation of occlusion of the chosen cortical vein, together with the intactness of other vessels, is a critical precondition for the validity of this model. For fluorescence angiography, an excitation source with a wavelength of 450–490 nm was used; at peak plasma concentrations of rose bengal, this might also cause photochemical damage. Because the half-life of circulating rose bengal is approximately 11 min (Pirotte, 1980), fluorescence angiography was performed before and 30 and 90 min after induction of venous occlusion. This approach did not cause brain damage or thrombosis induction in the sham-operated group.

The combination of the rose bengal photothrombosis technique with CBF monitoring using LDF scanning has distinct advantages. LD offers reliable, noninvasive, and continuous recordings of lCBF with high temporal resolution (Dirnagl et al., 1989; Skarphedinsson et al., 1989). However, CBF data are valid only for a spatially limited area (~1 mm^3) and are highly dependent on the localization of the LD probe. The fairly new LD scanning technique used here provides lCBF recordings from many defined locations by utilizing a motor-controlled micromanipulator. The excellent accuracy of repeated scans has been shown before (Ulrich et al., 1993; Ungersböck et al., 1993*b*). This way of analyzing LD data is useful, since it provides information on lCBF variability that is not available from a single stationary probe (Heimann et al., 1994). Moreover, the scanning procedure is helpful to minimize one of the shortcomings of the LD technique—i.e., the inability to express blood flow in absolute terms. Provided that enough locations are measured with the scanning technique, data thus obtained are not dimensioned on a completely arbitrary scale; with a very low and stable biological zero, the LD scale has a well-defined starting point.

A prerequisite to abandoning the term "arbitrary unit" is the use of a stable internal scale. With the current system, the internal scale is stable although not necessarily linear. The series of rats measured with the scanning technique so far (Ungersböck et al., 1993*b;* Heimann et al., 1994) clearly prove that cortical lCBF frequency histograms of individual animals compare well with the frequency histogram of the total population. The same has been shown for rabbit cortex (Kempski et al., 1995). Frequency histograms reveal the high spatial variability of lCBF; in our groups A and B, the median rCBF values were 56.5 and 54 LD units, respectively, with the 5% percentile at 22.1 and 22 LD units and the 95% percentile at 128 and 127 LD units, respec-

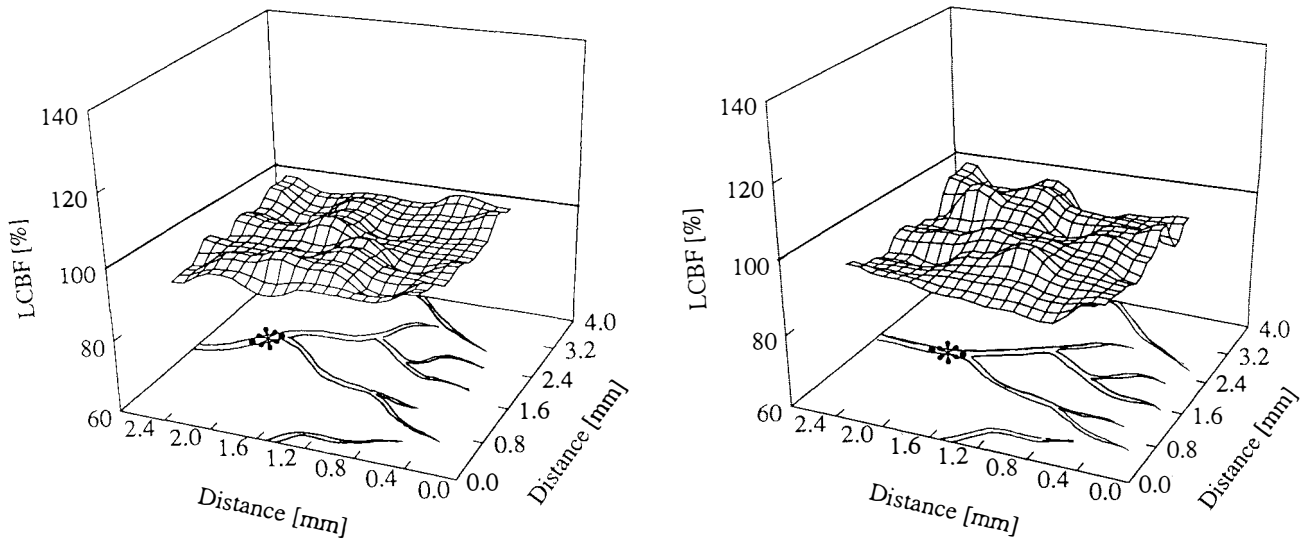

FIG. 6. A: Graph shows cortical CBF mapping 30 min after thrombus induction in a typical experiment (no. 20) from group A. Data are expressed as percentage changes from the individual baseline blood flow data collected at each location during the control phase. The location of the photochemically induced thrombus is indicated by an asterisk. The growing thrombus is indicated by black dots. The mapping demonstrates no changes in rCBF in this typical experiment. **B:** Cortical CBF mapping 90 min after thrombus induction in the same rat shows that the thrombus is not growing; no changes in rCBF were detected.

tively. This variability (obtained from 12 and five animals, respectively, from 48 locations each) compares well with that found with the umbelliferone technique (Anderson et al., 1992). Using that technique, Anderson et al. reported an average focal cortical flow in normocapnic rats of 49.7 ± 4.5 ml/100 g/min. The variability was 44% in normocapnia (Anderson et al., 1992). Flow was higher on the venous side than the arterial side. This finding corresponds well with our own observations, although the spatial resolution with the umbelliferone technique, with a measured area of 4.5 μm^2, was considerably better than that obtained with the LD technique (~1 mm^2). Other authors with different methods to assess lCBF found similar variabilities. Sako (1985), using a double-tracer autoradiographic technique, reported a 56% variability in 10 different locations, and Nakai et al. (1988) described 65% differences in five sites with triple-tracer autoradiography.

The value of the current results would be considerably enhanced if a topographical relationship between the rCBF changes and histopathological damage could be established; this would permit definition of critical thresholds for venous flow reductions. Unfortunately, this is currently not possible due to technical shortcomings. The experimental setup used here was primarily designed to collect regional LD data with high precision. A postmortem correlation of anatomy with observed flow changes would require a three-dimensional reconstruction from the serial sections with the ability to unmistakably identify landmarks on the cortical surface. Studies with new image-analysis equipment are currently planned.

After the localized venous occlusion, the more distal venous flow reverses. Cerebral veins, in contrast to peripheral veins, have no valves that would impede backward flow (Tsujimoto, 1990), so the direction of blood flow may change depending on the pressure gradients. Dilation of cerebral veins and recruitment of neighboring outflow territories may initially compensate for changes in pressure. Blood flow in veins with poor collateral flow, however, will become sluggish and may even come to a complete standstill, resulting in extension of the thrombus in some cases. The individual outcome, therefore, largely depends on the structure of collateral pathways and their capacity to maintain a sufficiently high flow to prevent thrombosis progression. If smaller branching veins become secondarily involved in the growing thrombus, pathological changes may develop, with extravasation of fluorescein into the brain around the occluded veins, indicating a breakdown of the blood–brain barrier. Fluorescence angiography permits direct observation of this chain of events.

Gotoh et al. (1993) have reported that occlusion of the SSS and diploic veins produced significant increases of intracranial pressure and CBVF, con-

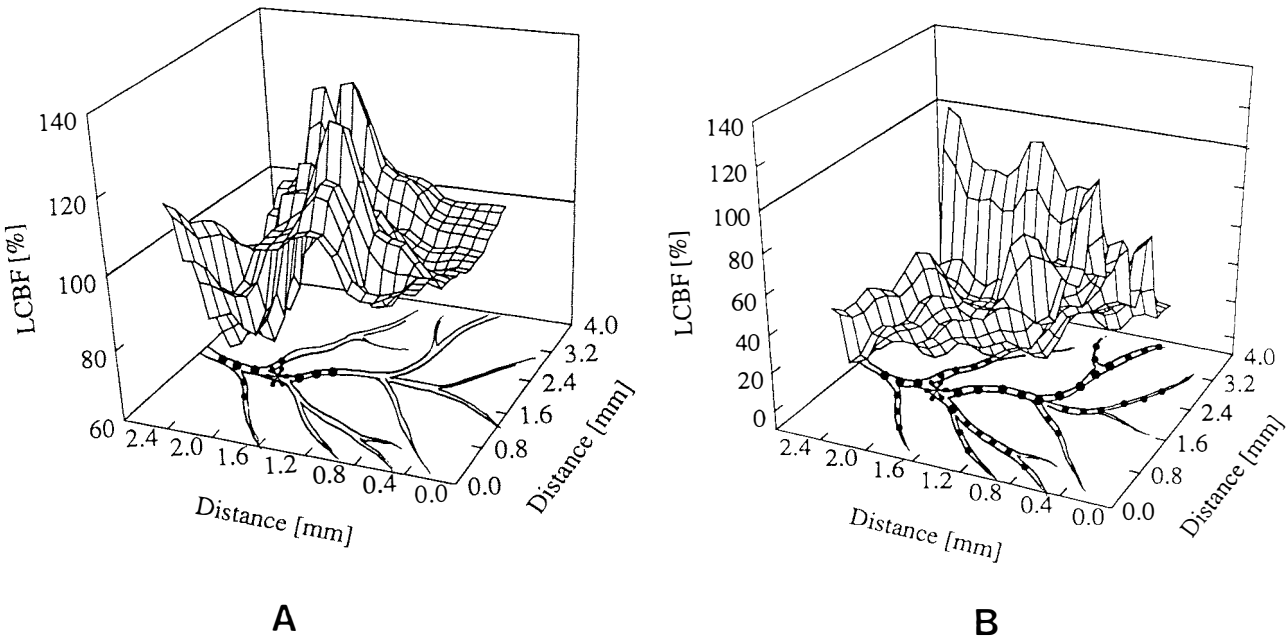

FIG. 7. A: Graph shows cortical CBF mapping 30 min after thrombus induction in a typical experiment (no. 6) from group B. The growing thrombus is indicated by black dots. The mapping reveals a hyperperfusion zone around a hypoperfused core area. **B:** In cortical CBF mapping 90 min after thrombus induction in the same animal, data are expressed as percentages of change from individual baseline values. The thrombus has grown, and the mapping shows a massive decrease in rCBF.

comitant with a decrease in rCBF and brain edema. Interestingly, our experiments revealed a temporary increase of CBVF 30 min after occlusion in group B (Fig. 4). Since the increase in CBVF regularly preceded the flow decrease, red cell velocity in the microcirculation was reduced at that time point—a condition that favors thrombosis expansion. It is consistent with this explanation that the elevated CBVF decreased again with a further reduction in rCBF after temporary blood pooling following venous occlusion.

The cortical CBF mapping revealed a gradual flow decrease in all animals from group B and transient hyperperfusion adjacent to areas of ischemia in three rats from group B. As depicted in Fig. 7, this hyperperfusion zone was found in an early stage following venous occlusion (in two cases at 15 min after occlusion and in one at 15 and 30 min) and changed to hypoperfusion at a later point in time. This low-flow zone developing around the venous thrombus persisted for a relatively long time. Although this is an extremely speculative suggestion, we believe that in the future the single-vein occlusion technique may be used as a model to study pathomechanisms in a penumbra-like tissue section (Strong et al., 1983). A penumbra-like situation with disturbed function but undisturbed structural metabolism might help us to understand the high variability of symptoms, including the often delayed functional recovery, in SVT patients.

Using fluorescence angiography and cortical LD scanning, we easily identified sequences of events after venous occlusions that defined two outcome groups (group A and B). The growth of the thrombus evidenced in group B coincided with a decrease in rCBF, a transient increase of CBVF, and moderate brain damage. It turned out that preservation of venous flow was considerable even if flow reversal occurred and that collateral pathways certainly play an important role in outcome. The growth of a venous thrombus can obstruct such pathways. Therefore, the clinical outcome subsequent to venous occlusion depends on the surrounding collateral reserve of the venous system. Brain damage subsequent to cortical vein occlusion can be predicted by lCBF monitoring and repeated angiography.

The present findings confirm that cerebral venous occlusion may cause local ischemia adjacent to occluded veins without sufficient collateral flow. This circulation perturbation appears even in the very early period following the venous occlusion and results in extension of a venous thrombus, local critical ischemia, and severe brain damage. Treatment paradigms such as heparin, thrombolysis (Barnwell et al., 1991), and venous revascularization (Sakaki et al., 1992) are appropriate as long as venous flow and CBF are not critically decreased.

Acknowledgment: The authors thank Monika Westenhuber for excellent secretarial assistance and Michael

Mahlzahn, Bärbel Kempski, Laszlo Kopacz, Andrea Schollmayer, and Angelica Karpi for the perfect technical help and support.

REFERENCES

Anderson RE, Meyer FB, Tomlinson FH (1992) Focal cortical distribution of blood flow and brain pH_i determined by in vivo fluorescent imaging. *Am J Physiol* 263:H565–H575

Barnwell SI, Higashida RT, Halbach VV, Dowd CF, Hieshima GB (1991) Direct endovascular thrombolytic therapy for dural sinus thrombosis. *Neurosurgery* 28:135–142

Beck DJK, Russell DS (1946) Experiments on thrombosis of the superior longitudinal sinus. *J Neurosurg* 3:337–347

Cervos-Navarro J, Kannuki S (1990) Neuropathological findings in the thrombosis of cerebral veins and sinuses—Vascular aspects. In: *Cerebral Sinus Thrombosis: Experimental and Clinical Aspects* (Einhäupl K, Kempski O, Baethmann A, eds), New York, Plenum Press, pp 15–26

Dirnagl U, Kaplan B, Jacewicz M, Pulsinelli W (1989) Continuous measurement of cerebral blood flow by laser-Doppler flowmetry in a rat stroke model. *J Cereb Blood Flow Metab* 9:589–596

Frerichs KU, Deckert M, Kempski O, Schürer L, Einhäupl K, Baethmann A (1994) Cerebral sinus and venous thrombosis in rats induces long-term deficits in brain function and morphology—Evidence for a cytotoxic genesis. *J Cereb Blood Flow Metab* 14:289–300

Fries G, Wallenfang T, Hennen J, Velthaus M, Heimann A, Schild H, Perneczky A, Kempski O (1992) Occlusion of the pig superior sagittal sinus, bridging and cortical veins: Multistep evolution of sinus-vein thrombosis. *J Neurosurg* 77: 127–133

Gotoh M, Ohmoto T, Kuyama H (1993) Experimental study of venous circulatory disturbance by dural sinus occlusion. *Acta Neurochir (Wien)* 124:120–126

Heimann A, Kroppenstedt S, Ulrich P, Kempski OS (1994) Cerebral blood flow autoregulation during hypobaric hypotension assessed by laser Doppler scanning. *J Cereb Blood Flow Metab* 14:1100–1105

Kanno T, Kasama A, Shoda M, Abe M (1992) Intraoperative monitoring on the occlusion of the venous system. *Neurosurgeons* 11:51–59 [in Japanese]

Kempski O, Heimann A, Strecker U (1995) On the number of measurements necessary to assess regional cerebral blood flow by local laser Doppler recordings: a simulation study with data from 45 rabbits. *Int J Microcirc* 15:37–42

Nakai H, Yamamoto YL, Diksic M, Worseley KJ, Takara E (1988) Triple-tracer autoradiography demonstrates effects of hyperglycemia on cerebral blood flow, pH, and glucose utilization in cerebral ischemia of rats. *Stroke* 19:764–772

Nakase H, Kakizaki T, Miyamoto K, Hiramatsu K, Sakaki T (1995) Prediction of brain damage subsequent to venous circulation disturbance by local cerebral blood flow monitoring—Cortical vein occlusion model by photochemical dye. *Neurosurgery* 37:280–286

Nakayama H, Dietrich WD, Watson BD, Busto R, Ginsberg MD (1988) Photothrombotic occlusion of rat middle cerebral artery: Histopathological and hemodynamic sequelae of acute recanalization. *J Cereb Blood Flow Metab* 8:357–366

Pirotte J (1980) Study of 131I-rose bengal kinetics in normal man; a critical evaluation of a three-compartment model. *Biomedicine* 32:17–21

Sakaki T, Hoshida T, Morimoto T, Tsunoda S, Tsujimoto S (1992) Cerebral venous disturbance and surgical treatment. *Neurosurgeons* 11:96–105 [in Japanese]

Sako K, Kobatake K, Yamamoto YL, Diksic M (1985) Correlation of local cerebral blood flow, glucose utilization, and tissue pH following a middle cerebral artery occlusion in the rat. *Stroke* 16:828–834

Sato S, Toya S, Ohtani M, Kawase T (1985) The effect of sagittal sinus occlusion on blood-brain barrier permeability and cerebral blood flow in the dog. In: *Brain Edema* (Inaba Y, Klatzo I, Spatz M, eds), Berlin, Heidelberg, New York, Tokyo, Springer, pp 235–239

Skarphedinsson JO, Harding H, Thorén P (1989) Repeated measurements of cerebral blood flow in rats. Comparison between the hydrogen clearance method and laser-Doppler flowmetry. *Acta Physiol Scand* 134:133–142

Strong AJ, Venables GS, Gibson G (1983) The cortical ischemic penumbra associated with occlusion of the middle cerebral artery in the cat. 1. Topography of changes in blood flow, potassium ion activity, and EEG. *J Cereb Blood Flow Metab* 3:86–96

Takeshima T, Miyamoto K, Okumura Y, Tominaga M, Tsujimoto S, Sakaki T (1993) Experimental study of local cerebral blood flow in cerebral venous occlusion. In: *Microcirculatory Stasis in the Brain* (Tomita M, Mchedlishvili G, Rosenblum, Heiss W-D, Fukuuchi Y, eds), Amsterdam, Elsevier Science, pp 441–444

Tsujimoto S (1990) A study of hemodynamics and pathological changes in circulatory disturbance due to venous occlusion. *J Nara Med Assoc* 41(2):159–181 [in Japanese]

Ulrich P, Kroppenstedt S, Marchand C, Heimann A, Kempski O (1993) Reserve capacity tested by acetazolamide response of cortical microflow up to six weeks after permanent bilateral occlusion of the common carotid artery of the rat. *J Cereb Blood Flow Metab* 13(suppl 1):S210

Ungersböck K, Heimann A, Kempski O (1993*a*) Cerebral blood flow alterations in a rat model of cerebral sinus thrombosis. *Stroke* 24:563–570

Ungersböck K, Heimann A, Strecker U, Kempski O (1993*b*) Mapping of cerebral blood flow by laser-Doppler flowmetry. In: *Microcirculatory Stasis in the Brain* (Tomita M, Mchedlishvili G, Rosenblum, Heiss W-D, Fukuuchi Y, eds), Amsterdam, Elsevier Science, pp 405–413

Watson BD, Dietrich WD, Prado R, Ginsberg MD (1987) Argon laser-induced arterial photothrombosis. *J Neurosurg* 66: 748–754